ACOUSTIC EQUALIZATION FOR HEADPHONES USING A FIXED FEED-FORWARD FILTER

Johannes Fabry, Fabio König, Stefan Liebich and Peter Jax

Institute of Communication Systems
RWTH Aachen University
Email: {fabry,koenig,liebich,jax}@iks.rwth-aachen.de

ABSTRACT

The headphones market is expanding and new applications based on active noise control (ANC) are emerging. In this contribution, we derive a fixed feed-forward FIR filter for ANC headphones based on a minimum mean-square error (MMSE) cost function that realizes user-defined active equalization and attenuation of the ambient sound. By analyzing the limit of this solution with respect to active attenuation, we derive a generalized solution that allows the user to influence the equalization even for high attenuation. We investigate the importance of *a priori* information and runtime measurements of the acoustic transfer functions, and show how this can be utilized to further increase the accuracy of the equalization.

Index Terms— Active noise control, causal Wiener filter, acoustic equalization

1. INTRODUCTION

The continuously rising level of environmental noise drives the need for countermeasures, which can hardly be satisfied by passive insulation. The broadly investigated technology of active noise control (ANC) is able to complement passive insulation to a great effect. Therefore, and due to new generations of audio processors, ANC headphones are experiencing a commercial success. Although the new processor technology is potent, the housing and power constraints of headphones are yet too demanding for feasible adaptive solutions in ANC headphones [1, 2].

The minimum mean-square error (MMSE) solution to fixed feed-forward FIR filters for ANC is given by the well known causal Wiener filter [3–5]. Feed-forward ANC systems benefit from guaranteed robustness and allow for attenuation of non-deterministic ambient sound. On the other hand, in order to design a robust feedback ANC system the variance of the secondary path needs to be considered [6, 7]. Furthermore, feedback ANC is only feasible for tonal noise and possibly in scenarios where no reference sensor is available. In this contribution, we modify the MMSE cost function to obtain an ANC system that allows for user-defined active equalization and attenuation of ambient sound. The concept of active acoustic equalization is used, e.g., in the field of occlusion reduction [8] or sound field control [9–11] with the target of achieving an acoustically transparent headphone or a flat magnitude response at the listening position with respect to the source. We investigate challenges that arise with the design of non-flat target transfer functions. In order to illustrate the flexibility of this approach, we previously designed a three-band parametric equalizer [12] with a variable attenuation as our target transfer function. Note, that the methods derived in this paper are optimal for any arbitrary target function. We further address challenges due to variation in the acoustic transfer functions of the ANC headphone [13] and show how *a priori* information and runtime measurements can be used to increase the accuracy of the overall transfer function.

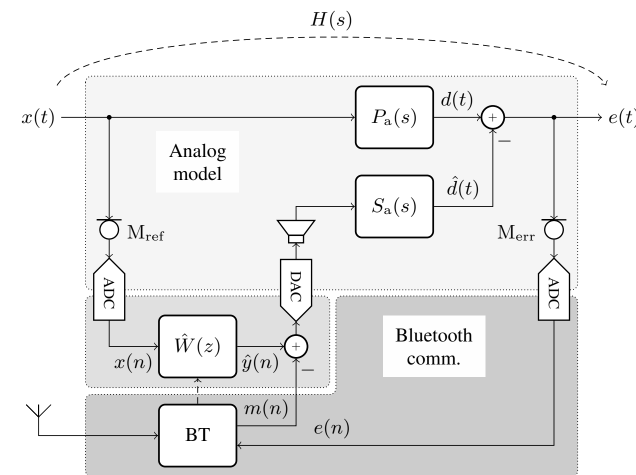

Fig. 1. Headphone topology with hardware components separated into an analog model ( ), a fast digital filter ( ), and Bluetooth (BT) communication ( ).

After a brief overview of the hardware setup, we derive the optimal equalization filter in Sec. 3. In Sec. 4 we show how the group delay of the secondary path should be considered in the target function and finally investigate the variance of the acoustic transfer functions in Sec. 5.

2. SYSTEM OVERVIEW

In the following, t and n denote the continuous and discrete time index. The arguments z and s refer to the z and Laplace transforms. Furthermore, bold uppercase $\boldsymbol{A}$ denotes a matrix and bold lowercase $\boldsymbol{a}$ denotes a vector. We define the z transform of a finite signal $\boldsymbol{a} = [a_0, a_1, \ldots, a_{N-1}]^{\mathrm{T}}$ of length N as $A(z) = \mathcal{Z}\{\boldsymbol{a}\}$, where the subscript on a_n is a compact form of the time index, i.e., $a_n = a(n)$.

Fig. 1 shows a hardware-related topology of ANC headphones. The analog model contains the reference microphone $\mathrm{M}_{\mathrm{ref}}$, which records the outer disturbance signal $x(t)$, the error microphone $\mathrm{M}_{\mathrm{err}}$, which records the error signal $e(t)$, and a loudspeaker, which plays back the compensation signal $\hat{y}(n)$ and the entertainment or measurement signal $m(n)$. The primary acoustic path $P_{\mathrm{a}}(s)$ describes the transfer function between $\mathrm{M}_{\mathrm{ref}}$ and $\mathrm{M}_{\mathrm{err}}$, whereas the secondary acoustic path $S_{\mathrm{a}}(s)$ describes the transfer function between the loudspeaker and $\mathrm{M}_{\mathrm{err}}$. The analog front-end is connected to the digital back-end through analog-to-digital converters (ADCs) and a digital-to-analog converter (DAC). The compensation signal $\hat{y}(n)$ is generated by filtering the discrete-time reference signal $x(n)$ with the equalization filter $\hat{W}(z)$. The filter coefficients of the equalization filter $\hat{W}(z)$ can be calculated on an external device, such as a smart phone, and transmitted via Bluetooth. Note that $\mathrm{M}_{\mathrm{err}}$ is not required to perform the equalization, but is essential for the design process and could be used to calibrate the secondary path at runtime. The signal $m(n)$ is optional and could be a measurement signal for identifying $S(s)$ or an entertainment signal. In the following, we assume that $m(n) = 0$. As we design a digital filter, we use discrete-time or z-domain notation for signals and impulse responses. Furthermore, $P(z)$ and $S(z)$ comprise the characteristics of the ADCs and the DAC, as well as the microphones and loudspeaker.

3. EQUALIZATION FILTER DESIGN

In this section, we derive the optimal time-invariant feed-forward equalization filter $\hat{W}(z)$ using a minimum mean-square error (MMSE) cost function. The solution is similar to the solution for pure ANC [3]. The objective is to design $\hat{W}(z)$ so that the overall transfer function $\hat{H}(z)$ of the ANC system matches an arbitrary target function $H(z)$:

$$P(z) - \hat{W}(z)S(z) = \hat{H}(z) \stackrel{!}{=} H(z) \tag{1}$$

The straightforward solution

$$W^{\mathrm{o}}(z) = \frac{P(z) - H(z)}{S(z)} \tag{2}$$

unfortunately, is not feasible since $S(z)$ is non-minimum-phase and therefore $W^{\mathrm{o}}(z)$ is anti-causal. In the following, we derive a causal approximation $\hat{\boldsymbol{w}} = [\hat{w}_0, \hat{w}_1, \ldots, \hat{w}_{L-1}]^{\mathrm{T}} \in \mathbb{R}^L$ of $W^{\mathrm{o}}(z)$ in the time-domain. We assume that all filters are time-invariant.

3.1. Wide-Band Solution

In this subsection, we derive the wide-band solution for the fixed feed-forward equalization filter $\hat{\boldsymbol{w}}$. We need to zero-pad the primary path vector $\boldsymbol{p}$ and the target function vector $\boldsymbol{h}$

$$\boldsymbol{p} = [p_0, p_1, \ldots, p_{L-1}, 0, \ldots, 0]^{\mathrm{T}} \in \mathbb{R}^{2L-1} \tag{3a}$$

$$\boldsymbol{h} = [h_0, h_1, \ldots, h_{L-1}, 0, \ldots, 0]^{\mathrm{T}} \in \mathbb{R}^{2L-1} \tag{3b}$$

so that their lengths are equal to the convolution product of $\hat{\boldsymbol{w}}$ and $\boldsymbol{s} = [s_0, s_1, \ldots, s_{L-1}]^{\mathrm{T}} \in \mathbb{R}^L$. To write the cost function in matrix notation, we define the convolution matrix

$$\boldsymbol{S} = \begin{bmatrix} s_0 & 0 & \ldots & 0 \\ s_1 & s_0 & \ddots & \vdots \\ \vdots & \vdots & \ddots & 0 \\ s_{L-1} & s_{L-2} & \ldots & s_0 \\ 0 & s_{L-1} & \ldots & s_1 \\ \vdots & \ddots & \ddots & \vdots \\ 0 & \ldots & 0 & s_{L-1} \end{bmatrix} \in \mathbb{R}^{2L-1 \times L} \tag{4}$$

of the secondary path $\boldsymbol{s}$ so that

$$\boldsymbol{S}\hat{\boldsymbol{w}} = \left[\hat{b}_0, \hat{b}_1, \ldots, \hat{b}_{2L-1}\right]^{\mathrm{T}} \in \mathbb{R}^{2L-1}, \tag{5a}$$

$$\hat{b}_n = \sum_{i=0}^{L-1} \hat{w}_i s_{n-i}. \tag{5b}$$

We now formulate the MMSE cost function with $\hat{\boldsymbol{h}} = \boldsymbol{p} - \boldsymbol{S}\hat{\boldsymbol{w}}$ and the differential vector $\boldsymbol{b} = \boldsymbol{p} - \boldsymbol{h}$ as

$$\mathcal{C}_{\mathrm{wb}} = \left\| \hat{\boldsymbol{h}} - \boldsymbol{h} \right\|^2 \tag{6a}$$

$$= \boldsymbol{b}^{\mathrm{T}}\boldsymbol{b} - 2\boldsymbol{b}^{\mathrm{T}}\boldsymbol{S}\hat{\boldsymbol{w}} + \hat{\boldsymbol{w}}^{\mathrm{T}}\boldsymbol{S}^{\mathrm{T}}\boldsymbol{S}\hat{\boldsymbol{w}}. \tag{6b}$$

By determining the minimum of $\mathcal{C}_{\mathrm{wb}}$ as a function of $\hat{\boldsymbol{w}}$

$$\frac{\partial \mathcal{C}_{\mathrm{wb}}}{\partial \hat{\boldsymbol{w}}} = -2\boldsymbol{S}^{\mathrm{T}}\boldsymbol{b} + 2\boldsymbol{S}^{\mathrm{T}}\boldsymbol{S}\hat{\boldsymbol{w}} \stackrel{!}{=} \boldsymbol{0}, \tag{7}$$

we find the optimal equalization filter

$$\hat{\boldsymbol{w}} = \left(\boldsymbol{S}^{\mathrm{T}}\boldsymbol{S}\right)^{-1} \boldsymbol{S}^{\mathrm{T}}\boldsymbol{b}. \tag{8}$$

This wide-band solution is a causal approximation of the optimal anti-causal equalization filter from (2). The matrix $\boldsymbol{\Psi}_{ss} = \boldsymbol{S}^{\mathrm{T}}\boldsymbol{S}$ is invertible, as it corresponds to the auto-correlation matrix of the secondary path $\boldsymbol{s}$ and is concentrated around its main diagonal.

3.2. Generalized Wide-Band Solution

The wide-band solution in (8) is implicitly capable of adjusting to target functions that comprise a scalar gain g. We can, for example, express the target function

$$\boldsymbol{h} = g\tilde{\boldsymbol{h}} \tag{9}$$

as the product of g and an arbitrary filter function $\tilde{\boldsymbol{h}}$. Writing $\hat{\boldsymbol{h}}$ using (8), (9), and the identity matrix $\boldsymbol{I}$ gives

$$\hat{\boldsymbol{h}} = \boldsymbol{p} - \boldsymbol{S}\hat{\boldsymbol{w}} \tag{10a}$$

$$= \left[\boldsymbol{I} - \boldsymbol{S}\left(\boldsymbol{S}^{\mathrm{T}}\boldsymbol{S}\right)^{-1}\boldsymbol{S}^{\mathrm{T}}\right]\boldsymbol{p} + g\boldsymbol{S}\left(\boldsymbol{S}^{\mathrm{T}}\boldsymbol{S}\right)^{-1}\boldsymbol{S}^{\mathrm{T}}\tilde{\boldsymbol{h}} \tag{10b}$$

and we observe that for small g the overall transfer function $\hat{\boldsymbol{h}}$ is independent of $\tilde{\boldsymbol{h}}$, which is counter-intuitive from a user point of view, as the user loses control over the shape of $\hat{H}(z)$.

In the following, we set up a generalized cost function and analyze its limit for high attenuation $g \to 0$. We observe that the limit of the generalized cost function corresponds to the minimization problem of a linear predictor, and utilize the property that the error signal is as flat as possible if the predictive filter is optimal. Finally, we find an artificial excitation signal $\hat{\boldsymbol{x}}$ that we consider for design of the equalization filter $\hat{\boldsymbol{w}}$ to preserve the shape of $H(z)$ in $\hat{H}(z)$, even for high attenuation. The resulting method is conceptually similar to a spectral weighting of an excitation signal for impulse response measurements [14].

In contrast to the impulse-response-based cost function (6) we now strive for a signal-based cost function. For now, we define an arbitrary excitation signal $\hat{\boldsymbol{x}} \in \mathbb{R}^M$ of finite length M. Its convolution matrix

$$\hat{\boldsymbol{X}} \in \mathbb{R}^{(M+2L-2)\times(2L-1)} \tag{11}$$

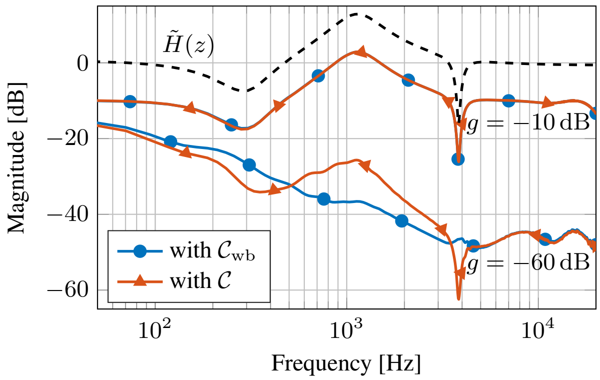

Fig. 2. Magnitude of spectrum $\hat{H}(z)$ for $\hat{\boldsymbol{w}}$ based on (6) and (13) with different gains g for $H(z)$ and $\tilde{H}(z)$ (- - -) as a reference.

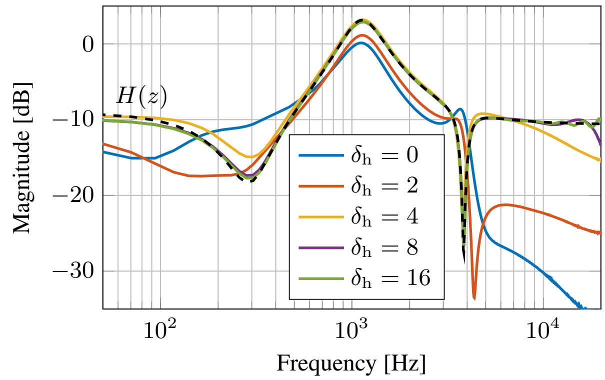

Fig. 3. Magnitude of spectrum $\hat{H}(z)$ for different values of additional group delay δ_{h} applied to the target function $H(z)$ (- - -).

is constructed similarly to (4) so that

$$\hat{\boldsymbol{X}}\boldsymbol{p} = \left[\hat{d}_0, \hat{d}_1, \ldots, \hat{d}_{M+L-1}, 0, \ldots, 0\right]^{\mathrm{T}} \in \mathbb{R}^{M+2L-2}, \quad (12a)$$

$$\hat{d}_n = \sum_{i=0}^{L-1} p_i \hat{x}_{n-i}. \quad (12b)$$

The generalized cost function is defined as

$$\mathcal{C} = \left\| \hat{\boldsymbol{X}} \left(\hat{\boldsymbol{h}} - \boldsymbol{h} \right) \right\|^2. \quad (13)$$

Note that $\boldsymbol{e} = \hat{\boldsymbol{X}}\hat{\boldsymbol{h}}$ corresponds to the output of the ANC system when $\hat{\boldsymbol{x}}$ is its input, and $\tilde{\boldsymbol{e}} = \hat{\boldsymbol{X}}\boldsymbol{h}$ corresponds to the target output.

In the following, we show how to determine $\hat{\boldsymbol{x}}$ so that the overall transfer function $\hat{H}(z)$ matches the shape of the target function $H(z)$. For high attenuation $g \to 0$ we obtain with (9) and (13)

$$\mathcal{C} \approx \left\| \hat{\boldsymbol{X}}\hat{\boldsymbol{h}} \right\|^2, \qquad \text{for } g \to 0, \quad (14)$$

which is minimal if the power of the system output $\boldsymbol{e}$ is minimal. Since a feed-forward ANC system is a linear predictor, the power of $\boldsymbol{e}$ is minimal if its magnitude spectrum is as flat as possible [15]. Assuming that the system output is approximately flat and scaled with a real-valued γ,

$$|E(z)| = \left| \hat{X}(z)\hat{H}(z) \right| \approx \gamma \quad (15)$$

and with $\hat{H}(z) \stackrel{!}{=} H(z)$ we choose

$$\hat{\boldsymbol{x}} = \mathcal{Z}^{-1}\left\{ \frac{\gamma}{|H(z)|} \right\} \quad (16)$$

so that $\hat{\boldsymbol{h}}$ minimizes $\boldsymbol{e}$ while considering the shape of $\boldsymbol{h}$.

The solution to minimizing the generalized cost (13) function for any gain g is given by

$$\hat{\boldsymbol{w}} = \left(\boldsymbol{S}^{\mathrm{T}} \boldsymbol{\Psi}_{\hat{x}\hat{x}} \boldsymbol{S} \right)^{-1} \boldsymbol{S}^{\mathrm{T}} \boldsymbol{\Psi}_{\hat{x}\hat{x}} \boldsymbol{b}, \quad (17)$$

where $\boldsymbol{\Psi}_{\hat{x}\hat{x}} = \hat{\boldsymbol{X}}^{\mathrm{T}}\hat{\boldsymbol{X}}$ denotes the auto-correlation matrix of $\hat{\boldsymbol{x}}$. If $\hat{\boldsymbol{x}}$ is uncorrelated, $\boldsymbol{\Psi}_{\hat{x}\hat{x}}$ corresponds to the identity matrix and the generalized solution (17) is equal to the wide-band solution (8). As $\boldsymbol{\Psi}_{\hat{x}\hat{x}}$ appears in the nominator and denominator of (17), the choice of $\hat{\boldsymbol{x}}$ is scale invariant, so we can choose $\gamma = 1$ in (16).

Fig. 2 illustrates how the generalized solution with an appropriate choice of $\hat{\boldsymbol{x}}$ influences the overall transfer function. We see that both methods behave similarly for $g = -10$ dB and that the wide-band solution no longer shapes $\hat{H}(z)$ accordingly for $g = -60$ dB. Since the wide-band solution is optimal, it follows that it is not possible to exceed its attenuation at all frequencies. We observed that increased attenuation at certain frequencies requires a reduced attenuation at other frequencies. This is similar to the water-bed effect, which is associated with Bode's integral for feedback control [16].

4. GROUP DELAY COMPENSATION

The secondary path is non-minimum-phase, and depending on its group delay, the first few filter taps of $\boldsymbol{b}$ can not be approximated by $\boldsymbol{S}\hat{\boldsymbol{w}}$ [8]. To illustrate the influence of an additional group delay $\delta_{\mathrm{s}} > 0$, we assume that $S(z)$ can be factored as

$$S(z) = z^{-\delta_{\mathrm{s}}} S_{\mathrm{m}}(z), \quad (18)$$

with a causal and invertible minimum-phase filter $S_{\mathrm{m}}(z)$. We insert (18) in (2) to obtain

$$W(z) = \frac{P(z) - H(z)}{z^{-\delta_{\mathrm{s}}} S_{\mathrm{m}}(z)} \quad (19a)$$

$$= z^{\delta_{\mathrm{s}}} \frac{P(z)}{S_{\mathrm{m}}(z)} - z^{\delta_{\mathrm{s}}} \frac{H(z)}{S_{\mathrm{m}}(z)}. \quad (19b)$$

Although the quotient is determinable because $S_{\mathrm{m}}(z)$ is invertible, we lose information by shifting the filter into the anti-causal plane by δ_{s} samples. Adding a group delay to a minimum-phase target function $H(z) = z^{-\delta_{\mathrm{h}}} H_{\mathrm{m}}(z)$ and with $\delta_{\mathrm{h}} = \delta_{\mathrm{s}}$ we partially compensate the group delay of $S(z)$ and obtain

$$W(z) = z^{\delta_{\mathrm{s}}} \frac{P(z)}{S_{\mathrm{m}}(z)} - \frac{H_{\mathrm{m}}(z)}{S_{\mathrm{m}}(z)}. \quad (20)$$

Fig. 3 shows how δ_{h} affects the overall transfer function $\hat{H}(z)$. Note that $P(z)$ and $S(z)$ used for generating Fig. 3 are calculated from measured data. Therefore, $S(z)$ only approximately fulfills the model assumption (18), as its group delay is frequency dependent. We observe that the overall transfer function $\hat{H}(z)$ is more accurate for larger δ_{h} and that it converges if δ_{h} exceeds the maximum group delay of $S(z)$. As the choice of the target function $H(z)$ is arbitrary, the results from this section can and should be considered in combination with the solutions from Sec. 3. For the rest of this paper we choose $\delta_{\mathrm{h}} = 8$, which in fact is also the case for Fig. 2.

5. VARIATIONS IN ACOUSTIC TRANSFER FUNCTIONS

From the previous sections, we know that knowledge of the electro-acoustic transfer functions $P(z)$ and $S(z)$ is essential for designing the equalization filter $\hat{\boldsymbol{w}}$. However, we can not assume perfect knowledge of the transfer functions.

In this section, we discuss how *a priori* information and runtime measurements of the acoustic paths can affect the performance of the ANC system. This concept is usually associated with the design of a feedback controller for ANC where variance of the secondary path needs to be considered to ensure robustness [6], [7]. We consider a multitude of J measurements $\boldsymbol{p}_j$ of the primary path and $\boldsymbol{s}_j$ of the secondary path with $j = 0, \ldots, J-1$, that are performed prior to the design of $\hat{\boldsymbol{w}}$. These measurements deviate from the average paths

$$\overline{\boldsymbol{p}} = \frac{1}{J}\sum_{j=0}^{J-1} \boldsymbol{p}_j, \qquad \overline{\boldsymbol{s}} = \frac{1}{J}\sum_{j=0}^{J-1} \boldsymbol{s}_j \tag{21}$$

by

$$\boldsymbol{p}_j = \overline{\boldsymbol{p}} + \Delta\boldsymbol{p}_j \tag{22a}$$

$$\boldsymbol{s}_j = \overline{\boldsymbol{s}} + \Delta\boldsymbol{s}_j. \tag{22b}$$

We assume that each pair of $\boldsymbol{p}_j$ and $\boldsymbol{s}_j$ is measured simultaneously. To find the equalization filter $\hat{\boldsymbol{w}}$ that yields the optimal averaged performance for a multitude of J previously measured acoustic paths, we modify the cost function (13) which, with $\hat{\boldsymbol{h}}_j = \boldsymbol{p}_j - \boldsymbol{S}_j\hat{\boldsymbol{w}}$, results in

$$\overline{C} = \sum_{j=0}^{J-1} \left\| \hat{\boldsymbol{X}} \left(\hat{\boldsymbol{h}}_j - \boldsymbol{h} \right) \right\|^2. \tag{23}$$

The convolution matrix $\hat{\boldsymbol{X}}$ is constructed with $\hat{\boldsymbol{x}}$ chosen according to (16). We obtain the optimal equalization filter with $\boldsymbol{b}_j = \boldsymbol{p}_j - \boldsymbol{h}$ as

$$\hat{\boldsymbol{w}}\left(\overline{\boldsymbol{p}}, \overline{\boldsymbol{s}}\right) = \left(\sum_{j=0}^{J-1} \boldsymbol{S}_j^{\mathrm{T}} \boldsymbol{\Psi}_{\hat{x}\hat{x}} \boldsymbol{S}_j \right)^{-1} \sum_{j=0}^{J-1} \boldsymbol{S}_j^{\mathrm{T}} \boldsymbol{\Psi}_{\hat{x}\hat{x}} \boldsymbol{b}_j. \tag{24}$$

For a statistically significant number of J *a priori* data, the equalization filter from (24) should yield near optimal performance, even for a test set with $K \gg J$ measurements.

To further increase the performance, we might measure the actual transfer functions $\boldsymbol{p}$ and $\boldsymbol{s}$ at runtime. A runtime measurement of $\boldsymbol{s}$ is feasible, as we can play back a measurement signal $m(n)$ via the internal loudspeaker of the headphone, as Fig. 1 illustrates. Furthermore, the ANC system increases the SNR at the error microphone since it decreases the energy of the inner disturbance signal $d(n)$. On the other hand, acquiring $\boldsymbol{p}$ at runtime is error-prone, as we either have no influence on the measurement signal and SNR or require an external playback device and a quiet environment. Therefore, we only evaluate the case in which we have perfect knowledge of $\boldsymbol{s}$. For now, we assume that $\boldsymbol{p}$ and $\boldsymbol{s}$ are independent. With a measurement of the secondary path $\boldsymbol{s}$, we can simplify (24) to

$$\hat{\boldsymbol{w}}\left(\overline{\boldsymbol{p}}, \boldsymbol{s}\right) = \left(\boldsymbol{S}^{\mathrm{T}} \boldsymbol{\Psi}_{\hat{x}\hat{x}} \boldsymbol{S} \right)^{-1} \boldsymbol{S}^{\mathrm{T}} \boldsymbol{\Psi}_{\hat{x}\hat{x}} \left(\overline{\boldsymbol{p}} - \boldsymbol{h} \right). \tag{25}$$

In order to evaluate the effect of acoustic path knowledge on the performance, we measured the overall transfer function $\hat{H}$ for $J = 12$ participants in a studio box using a Neumann KH 120 speaker in a lateral position. We used a modified Bose QC20 headphone as an electro-acoustic front-end. The digital back-end was provided by a dSPACE real-time system. The gain is set to $g = -10\,\mathrm{dB}$ and the delay was chose as $\delta_{\mathrm{h}} = 8$. We extended the target function $H(z)$ by an additional high-cut filter at 8 kHz since the uncertainties above that frequency range prohibit good performance under real test conditions.

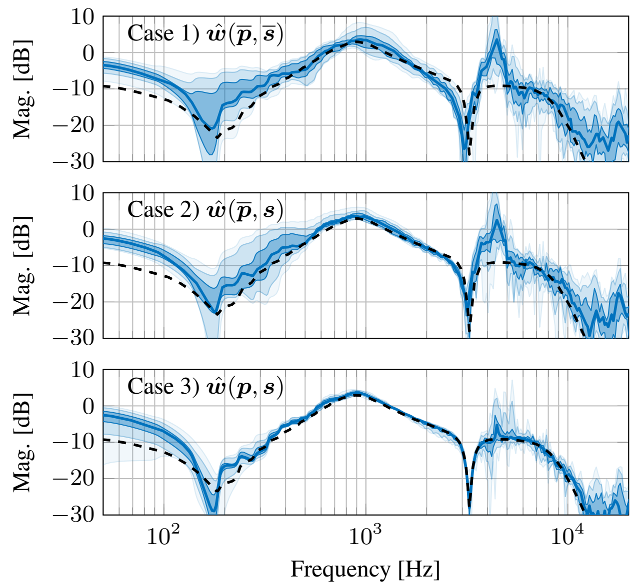

Fig. 4. Tubes of 100% ( ), 80% ( ) and 50% ( ) confidence with median ( ) of $\hat{H}(z)$ and target function $H(z)$ ( ).

Fig. 4 shows tubes of confidence of the measured overall transfer functions $\hat{H}(z)$ for equalization filters based on different knowledge of the primary path $\boldsymbol{p}$ and secondary path $\boldsymbol{s}$. In the first case, neither the actual $\boldsymbol{p}$ nor $\boldsymbol{s}$ are known and the control filter is based on the average according to (24). In the second case, the secondary path is measured by playing back an exponential sweep via the internal loudspeaker. The equalization filter is calculated according to (25). In the third case, the secondary path was measured as previously described and the primary path was measured by playing back an exponential sweep over an external loudspeaker. The equalization filter is calculated according to (17). The benefit of knowing the actual transfer paths is apparent. For the second case, we clearly see improvements in comparison to the first case at around 200 Hz, as well as a better alignment of the notch filter at 3.2 kHz. The deviation between 3.6 kHz and 4.7 kHz is due to a resonance of the loudspeaker and can only be compensated with perfect knowledge of $\boldsymbol{p}$ and $\boldsymbol{s}$, as seen for the third case.

6. CONCLUSION

In this contribution, we proposed different MMSE-based solutions for designing a fixed feed-forward FIR filter for an ANC headphone that allows for user-defined equalization and attenuation of ambient sound. We improved on the straightforward solution by analyzing the limit of its overall transfer function with respect to the active attenuation. Furthermore, we considered the group delay of the secondary path as well as *a priori* information and measurements of the acoustic transfer functions to increase the accuracy of the overall transfer function with respect to the target function. The observations and numerical results are based on actual measurements.

7. REFERENCES

[1] J. Fabry, S. Liebich, P. Vary, and P. Jax, "Active noise control with reduced-complexity Kalman filter," in *16th International Workshop on Acoustic Signal Enhancement (IWAENC)*. IEEE, Sep. 2018.

[2] M. Zhang, H. Lan, and W. Ser, "Cross-updated active noise control system with online secondary path modeling," *IEEE Trans. Speech Audio Process.*, vol. 9, no. 5, pp. 598–602, Jul. 2001.

[3] S. M. Kuo and D. R. Morgan, *Active Noise Control Systems: Algorithms and DSP Implementations*. Hoboken: Wiley, 1996.

[4] S. Elliott, *Signal Processing for Active Control*. Amsterdam, Netherlands: Elsevier, 2000.

[5] C. Hansen, S. Snyder, X. Qiu, L. Brooks, and D. Moreau, *Active Control of Noise and Vibration*. Boca Raton: CRC Press, 2012.

[6] Y. Song, Y. Gong, and S. M. Kuo, "A robust hybrid feedback active noise cancellation headset," *IEEE Trans. Speech Audio Process.*, vol. 13, no. 4, pp. 607–617, Jul. 2005.

[7] S. Liebich, C. Anemüller, P. Vary, P. Jax, D. Rüschen, and S. Leonhardt, "Active noise cancellation in headphones by digital robust feedback control," in *24th European Signal Processing Conference (EUSIPCO)*. EURASIP, 2016, pp. 1843–1847.

[8] S. Liebich, R. Brandis, J. Fabry, P. Jax, and P. Vary, "Active occlusion cancellation with hear-through equalization for headphones," in *Proc. IEEE International Conference on Acoustics, Speech and Signal Processing (ICASSP)*, 2018, pp. 241–245.

[9] M. Bouchard, "Multichannel affine and fast affine projection algorithms for active noise control and acoustic equalization systems," *IEEE Trans. Speech Audio Process.*, vol. 11, no. 1, pp. 54–60, 2003.

[10] J. Rämö, V. Välimäki, and M. Tikander, "Live sound equalization and attenuation with a headset," in *51st International Conference: Loudspeakers and Headphones*. Audio Engineering Society, 2013.

[11] F. Denk, M. Hiipakka, B. Kollmeier, and S. M. A. Ernst, "An individualised acoustically transparent earpiece for hearing devices," *Int. J. Audiol.*, vol. 57, no. sup3, pp. S62–S70, 2018.

[12] S. J. Orfanidis, "Digital parametric equalizer design with prescribed Nyquist-frequency gain," *J. Audio Eng. Soc.*, vol. 45, no. 6, pp. 444–455, 1997.

[13] S. Liebich, J. Fabry, P. Jax, and P. Vary, "Signal processing challenges for active noise cancellation headphones," in *ITG-Fachtagung Sprachkommunikation*, VDE. VDE Verlag GmbH, Oct. 2018.

[14] S. Müller and P. Massarani, "Transfer-function measurement with sweeps," *J. Audio Eng. Soc.*, vol. 49, no. 6, pp. 443–471, 2001.

[15] P. Vary and R. Martin, *Digital Speech Transmission: Enhancement, Coding and Error Concealment*. Hoboken: Wiley, 2006.

[16] K. J. Åström, "Limitations on control system performance," *European J. Contr.*, vol. 6, no. 1, pp. 2–20, 2000.